RESEARCH ARTICLE

Pterostilbene induces autophagy and apoptosis in sensitive and chemoresistant human bladder cancer cells

Rong-Jane Chen[1], Chi-Tang Ho[2] and Ying-Jan Wang[1]

[1] Department of Environmental and Occupational Health, National Cheng Kung University Medical College, Tainan, Taiwan
[2] Department of Food Science, Rutgers University, New Brunswick, NJ, USA

Received: February 4, 2010
Revised: May 13, 2010
Accepted: May 17, 2010

Scope: Bladder cancer is one of the most common malignancies in the world. The majority of bladder cancer deaths are due to unresectable lesions that are resistant to chemotherapy. Pterostilbene (PT), a naturally occurring phytoalexin, possesses a variety of pharmacologic activities, including antioxidant, cancer prevention activity and cytotoxicity to many cancers. We found that PT effectively inhibits the growth of sensitive and chemoresistant human bladder cancer cells by inducing cell cycle arrest, autophagy and apoptosis. Down-regulations of Cyclin A, B and D1 and pRB are the results of PT-induced cell cycle arrest.

Methods and results: Autophagy occurred at an early stage and was observed through the formation of acidic vesicular organelles (the marker for autophagy) and microtubule-associated protein 1 light chain 3-II production. Apoptosis occurred at a later stage and was detected by Annexin V and 4′,6-diamidino-2-phenylindole staining. PT-induced autophagy was triggered by the inhibition of active human protein kinase/the mammalian TOR/p70S6K pathway and activation of extracellular signal-regulated kinase pathway. Inhibition of autophagy by pretreatment with 3-methyladenine, bafilomycin A1, *Beclin 1* or *extracellular signal-regulated kinase* short hairpin RNA enhanced PT-triggered apoptosis.

Conclusion: This is the first study to demonstrate that PT causes autophagy in cancer cells and suggests that PT could serve as a new and promising agent for the treatment of sensitive and chemoresistant bladder cancer cells.

Keywords:
Apoptosis / Autophagy / Cell cycle arrest / Chemoresistance / Pterostilbene

1 Introduction

In the United States, bladder cancer is the fourth most common malignancy in men and the ninth most common in women. Bladder cancer is characterised by frequent recurrence and poor clinical outcome when tumours from noninvasive flat and papillary urothelial neoplasia invade muscle or metastasis [1]. The majority of deaths from bladder cancer are due to advanced, unresectable lesions that are resistant to chemotherapy [2]. Chemoresistance in bladder cancer is associated with cigarette smoking and may be due to long-term nicotine exposure [3]. We previously reported that nicotine-induced defects in apoptosis machinery lead to chemoresistance in human bladder cancer cells [4]. There is a need to identify new chemotherapeutic agents and/or new cytotoxic strategies

Correspondence: Dr. Ying-Jan Wang, Department of Environmental and Occupational Health, National Cheng Kung University Medical College, 138 Sheng-Li Road, Tainan 70428, Taiwan
E-mail: yjwang@mail.ncku.edu.tw
Fax: +886-6-275-2484

Abbreviations: 3-MA, 3-methyladenine; **AKT,** active human protein kinase; **AVO,** acidic vesicular organelle; **BafA1,** bafilomycin A1; **Cis,** cisplatin; **DAPI,** 4′,6-diamidino-2-phenylindole; **ERK1/2,** extracellular signal-regulated kinase; **IC_{50},** drug concentration that inhibits cell growth by 50%; **LC3,** microtubule-associated protein 1 light chain 3; **mTOR,** mammalian TOR; **MTT,** 3-(4,5-dimethylthiazol-2-yl)-2,5-diphenyltetrazolium bromide; **PI3K,** phosphatidylinositol-3-kinase; **PT,** pterostilbene; **shRNA,** short hairpin RNA; **Tax,** paclitaxel

that will combat chemoresistant bladder cancer cells that have defects in apoptosis.

Pterostilbene (PT) (*trans*-3,5-dimethoxy-4′-hydroxystilbene) is a naturally occurring phytoalexin identified in several plants in the genus *Pterocarpus*, in *Vitis vinifera* leaves, in some berries (*e.g.* blue berries and cranberries), and in grapes [5]. PT has diverse pharmacologic activities including antioxidant activity, cancer prevention activity [5] and the ability to inhibit DNA synthesis [6]. It is also cytotoxic *in vitro* to a number of cancer cell lines, including breast cancer, melanoma, colon, liver and gastric cancer cells [5, 7, 8]. The ability of PT to induce apoptosis in sensitive and drug-resistant lymphoma cell lines has been examined *in vitro* [9]. Although PT exerts antiproliferative and proapoptotic activities in various cancer cell types, the underlying mechanisms of autophagy remain unclear. In addition, the effects of PT on bladder cancer cells are unknown.

Cell death can result from distinct processes, namely apoptosis (type I cell death) and autophagy (type II cell death). Autophagy is morphologically distinct from apoptosis and is characterised by the accumulation of autophagic vacuoles in the cytoplasm that surround a normal nucleus [10]. Autophagy preserves cell survival under unfavourable conditions by ensuring lysosomal degradation of aged or damaged proteins, membranes and cytosolic structures [11]. Recently, extensive attention has been paid to the role of autophagy in cancer development and therapy [12–14]. The relationship between apoptosis and autophagy is complex and varies between cell types and different stresses. Certain agents kill cancer cells through nonapoptotic pathways and may circumvent chemoresistance. Such agents may be promising for treating resistant cancers [15]. For this reason, tumour cells with defects in apoptosis undergo autophagy, and inhibition of autophagy causes tumour cells to die through alternative mechanisms [16]. It has also been suggested that autophagy may provide a useful way to prevent cancer development, limit tumour progression and enhance the efficacy of cancer treatments [17].

Two main signalling pathways that regulate autophagy are phosphatidylinositol-3-kinase (PI3K)/active human protein kinase (AKT)/mammalian TOR (mTOR) and MEK/extracellular signal-regulated kinase (ERK1/2) [17]. Activation of class I PI3K inhibits autophagy through activation of the AKT/mTOR pathway. Conversely, activation of class III PI3K in a complex with Beclin 1 promotes autophagy [18]. The Raf-1/MEK1/2/ERK1/2 pathway also mediates autophagy. ERK1/2 phosphorylates the Gα-interacting protein, which accelerates GTP hydrolysis through the Gαi3 protein, resulting in the induction of autophagy [19]. MAPK/ERK1/2 activation is also essential in autophagy induced by curcumin [20], arsenic trioxide [12] or lindane [21].

In this study, we investigated the anticancer effect of PT on sensitive and nicotine-induced chemoresistant bladder cancer cells. Interestingly, we found that PT effectively inhibits the growth of both cell types by inducing autophagy, apoptosis and cell cycle arrest. We examined the mechanisms underlying PT-induced autophagy and studied the relationship between PT-induced autophagy and apoptosis. To the best of our knowledge, this is the first study to demonstrate that PT induces autophagy, which is regulated by the simultaneous inhibition of the AKT/mTOR/p70S6K pathway and stimulation of the ERK1/2 pathway. These data emphasise the role of autophagy in the cellular response to PT and suggest that the optimisation of its anticancer activity can be achieved through autophagy pathways.

2 Materials and methods

2.1 Cell culture and chemicals

The T24 human bladder cancer cell line was purchased from ATCC (ATCC: HTB-4) (ATCC: American Type Culture Collection, Manassas, VA, USA). T24 cells were maintained in 10 cm^2 dishes in McCoy 5A medium (Sigma-Aldrich, St. Louis, MO, USA) supplemented with 100 U/mL penicillin, 100 μg/mL streptomycin (Gibco) and 10% heat-inactivated fetal calf serum (HyClone). The T24R chemoresistant human bladder cancer cell line cells were established by long-term nicotine exposure [4]. PT was provided by Chi-Tang Ho (Department of Food Science, Rutgers University) and Dr. Min-Hsiung Pan (Department of Seafood Science, National Kaohsiung Marine University). The purity of PT is 96%.

3-(4,5-Dimethylthiazol-2-yl)-2,5-diphenyltetrazolium bromide (MTT), cisplatin (Cis), paclitaxel (Tax), 3-methyladenine (3-MA), bafilomycin A1 (BafA1) and 4′,6-diamidino-2-phenylindole (DAPI) were purchased from Sigma-Aldrich. The ERK1/2 inhibitor U0126 and the PI3K/AKT inhibitor (LY294002) were obtained from Cell Signaling (Beverly, MA, USA). Acridine orange was purchased from USB. The general caspase inhibitor Z-VAD-FMK was obtained from R&D Systems (Minneapolis, MN, USA). Antibodies against Cyclin D1, Cyclin A, Cyclin B, phospho-Rb, Bcl-2, Bax, Bad, Bcl-xl, Beclin 1, ERK1/2, phospho-ERK1/2, AKT, phospho-AKT, phospho-p70S6K, GAPDH and horseradish peroxidase-conjugated anti-mouse and anti-rabbit secondary antibodies were purchased from Cell Signaling. The anti-microtubule-associated protein 1 light chain 3 (LC3) antibody was obtained from MBL, and the p70S6K antibody was purchased from Transduction (BD Biosciences). Pro Caspase-3 and cleaved Caspase-3 antibodies were purchased from Epitomics (Burlingame, CA, USA).

2.2 Cell viability assay

Cells were seeded in a 96-well plate at a density of 2×10^3 cells/well and incubated overnight. After removing the medium, 100 μL of anti-tumour agent was added, and cells were harvested at the indicated time points. Next, 100 μL of MTT was added to the wells, and the plate was incubated for

2 h at 37°C. The medium was removed and 100 μL of DMSO was added to the wells. Absorbance was measured at 570 nm using an ELISA plate reader.

2.3 Detection of cell death

According to updated NCCD (Nomenclature Committee on Cell Death) guidelines [22], cell death can be detected by the use of various methods. These methods include visualising morphological changes under phase-contrast microscopy, and analysing PI exclusion by flow cytometry. Briefly, cells were collected, washed with PBS, stained with PI (50 μg/mL) at 37°C for 30 min and analysed by flow cytometry.

To analyse cell viability, cells were seeded in a 96-well plate at a density of 2×10^3 cells/well and incubated overnight. After removing the medium, 100 μL of anti-tumour agent was added and cells were harvested at the indicated time points. Next, MTT (100 μL) was added to the wells, and the plate was incubated for 2 h at 37°C. The medium was removed and 100 μL of DMSO was added to the wells. Absorbance was measured at 570 nm using an ELISA plate reader.

2.4 Annexin V and PI staining assay

One of the early characteristics of apoptosis is the rapid translocation and accumulation of the membrane phospholipid phosphatidylserine from the cytoplasmic interface to the extracellular surface. Annexin V has a high affinity for phosphatidylserine and is used as an indicator of apoptosis. Cells were trypsinised, washed with 1 × PBS and centrifuged at 3000 rpm for 5 min. Cells were resuspended in 100 μL of 1 × Annexin V-binding buffer (10 mM HEPES (pH 7.4), 0.14 M NaCl and 2.5 mM $CaCl_2$) that contained 5 μL of Annexin V-FITC (Becton Dickinson, San Jose, CA, USA) alone or in combination with 10 μL of PI (50 μg/mL) and were incubated at room temperature for 15 min. The 1 × binding buffer (400 μL) was added to stop the reaction, and the staining was analysed by flow cytometry.

2.5 DAPI stain

Apoptosis was quantified by counting the number of cells containing nuclear changes with apoptotic characteristics, such as chromatin condensation and nuclear fragmentation after DAPI staining. In brief, cells were collected and stained with DAPI (1 μg/mL) for 15 min. After incubation, cells were examined by fluorescence microscopy using excitation and emission filters of 380 and 430 nm, respectively. Each treatment was repeated at least three times, and 100 cells were counted for each treatment.

2.6 Cell cycle analysis

Cells were washed with 1 × PBS, trypsinised and fixed with 75% ethanol for at least 4 h. After fixation, the cells were washed with 1 × PBS and stained with 4 μg/mL PI for 30 min. PI immunofluoresence was measured with FACScan (Becton Dickinson). The percentage of cells below the G1 peak (subG0/G1 fraction) and the distribution of cells in the cell cycle were analysed using WinMDI software.

2.7 Caspase 3 activity assay

Caspase 3 activity was quantified using a Caspase Fluorometric Assay Kit (R&D Systems) according to the manufacturer's instructions. Following a 48 h treatment of PT, cell extracts (100 μg) were incubated with the caspase substrate for 1 h at 37°C. Caspase-specific peptides that are conjugated to the fluorescent reporter molecule 7-amino-4-trifluromethyl coumarin were added to the reaction and incubated at 37°C for 1–2 h. The cleavage of peptide by Caspase 3 releases free 7-amino-4-trifluromethyl coumarin that was quantified using a fluorescence spectrophotometer (400 nm excitation and 505 nm emission).

2.8 Detection and quantification of acidic vesicular organelles with acridine orange staining

Autophagy is the process of sequestering cytoplasmic proteins into the lytic components, and it is characterised by the formation of acidic vesicular organelles (AVOs) as described previously [23]. Cells were treated with PT for 48 h and vital staining with AO was performed. To quantify the development of AVOs, cells were harvested and stained with 1 μg/mL acridine orange for a period of 20 min and analysed by a fluorescence microscope (Axioscop) equipped with a mercury 100 W lamp, 490 nm band-pass blue excitation filters, a 500 nm dichroic mirror and a 515 nm long-pass barrier filter. Flow cytometric analysis was also used to detect AVO percentages [24].

2.9 Electron microscopy

Cells were fixed with a solution containing 2.5% glutaraldehyde and 2% paraformaldehyde (in 0.1 M cacodylate buffer, pH 7.3) for 1 h. After fixation, the samples were postfixed for 30 min in the same buffer containing 1% OsO_4. Ultra-thin sections were observed under a transmission electron microscope (JEOL JEM-1200EX, Japan) at 100 kV.

2.10 Western blot analysis

The isolation of total cellular lysates, immunoprecipitation, gel electrophoresis and immunoblotting were performed

according to the methods described previously [25]. Immunoreactive proteins were visualised with the ECL chemiluminescent detection system (PerkinElmer Life Science, MA, USA) and BioMax LightFilm (Eastman Kodak, New Heaven, CT, USA) according to the manufacturer's instructions.

2.11 RNA interference

We used the MicroPorator, a pipette-type electroporation system, (Digital Bio Tech., Korea) to transfect cells. The RNA interference reagents were obtained from the National RNA interference Core Facility located at the Institute of Molecular Biology/Genomic Research Centre, Academia Sinica, supported by the National Research Program for Genomic Medicine Grants of NSC (NSC 97-3112-B-001-016). The human library is referred to as TRC-Hs 1.0. Individual clones are identified as short hairpin RNA (shRNA) TRCN0000010997, shRNA TRCN0000010040 and shRNA TRCN0000072178, shRNA TRCN0000072196 and shRNA TRCN0000033550.

2.12 Statistical analysis

Results are expressed as mean $\pm$ SEM. Experimental data were analysed using the Student's *t*-test. Differences were considered to be statistically significant when the *p*-value was less than 0.05. Data in Figs. 6C and D are analysed by ANOVA followed by the Bonferroni *t*-test for pairwise multiple comparisons.

3 Results

3.1 PT inhibits growth in bladder cancer cell lines

Chemoresistant T24R cells were established by long-term nicotine treatment of T24 cells [4]. To confirm the resistance in the T24R cells, T24 and T24R cells were exposed to different concentrations of Cis or Taxfor 1–3 days. As shown in Figs. 1A and B, Cis and Tax effectively inhibited cell growth in sensitive T24 cells, but T24R cells were more resistant to Cis and Tax. We then tested the antiproliferative effect of PT in both cell lines. T24 and T24R cells were treated with 50, 75 and 100 μM PT for 1–3 days. PT significantly decreased the growth of sensitive and chemoresistant bladder cancer cells in a concentration- and time-dependent manner (Figs. 1C and D). To compare the antiproliferative activity of PT in T24 and T24R cells, the drug concentration that inhibits cell growth by 50% (IC_{50}) was calculated. The IC_{50} after 48 h of PT treatment is 66.58 ± 1.84 and 77.95 ± 0.44 μM in sensitive T24 cells and chemoresistant T24R cells, respectively. PT induces cell death at 24 h by necrosis (Annexin V-negative, PI-positive) then decreased at 48 and 72 h, meanwhile apoptosis (Annexin V and PI-positive) was increased in both cell types (Fig. 1E). Following PT treatment, T24 cells did not condense, whereas the cytoplasm and cell surface developed highly granular appearances (Fig. 1F).

3.2 PT induces changes in cell cycle distribution and apoptosis in T24 and T24R cells

We next examined the effects of PT on the cell cycle distribution of both cells. Treatment with PT for 24 h induced a marked increase in the G0/G1 phase and a decrease in the G2/M phases as compared with controls (Fig. 2A). S-phase arrest (through DNA replication inhibition) occurs at lower concentrations (50 and 75 μM) of PT (Fig. 2A). The PT (100 μM)-induced G0/G1 arrest shifted to an S-phase arrest at 48 and 72 h. During this time, there was a time-dependent increase in the number of cells in subG0/G1 phase and was a decrease of cells in G2/M phase (Fig. 2B). The results indicated that PT delayed cell cycle progression in both cell types. Therefore, PT-induced cell cycle arrest likely contributed to the overall growth suppression in T24 and T24R cells.

In addition to cell cycle arrest, we used several apoptosis markers to investigate whether PT induces cell death by apoptosis. Following treatment with PT, the percentage of cells in subG0/G1 increased in a concentration- (Fig. 2A) and time- (Fig. 2B) dependent manner in both cell lines. We next analysed surface exposure of phosphatidylserine, an early event in apoptosis by Annexin V staining. The percentage of cells staining positive for Annexin V was slightly increased in both cells types after 24 h of PT treatment but was much higher following 72 h of treatment (Fig. 2C). Caspase-3 activity also increased significantly at 72 h (Fig. 2D). To examine apoptosis morphologically, the nuclei of treated T24 and T24R cells were stained with DAPI at 24, 48 and 72 h and observed by fluorescence microscopy (Supporting Information Fig. S1A). Apoptotic cells with morphological characteristics, such as chromatin condensation and nuclear fragmentation, were counted and are shown in Fig. 2E. The results show that increased apoptosis in control cells at 72 h may be due to cell confluence. However, apoptosis in both cell types were evident following PT treatment, and apoptosis peaked at 72 h.

The effects on cell cycle regulatory proteins were analysed using western blot analysis. Cyclin A, B and D1 and pRb were inhibited in a concentration- and time-dependent manner in both cell types (Figs. 3A and B). The levels of pRb decreased 6 h after PT treatment, and this effect continued until 48 h. This indicates that inactivation of pRb could be induced by PT in T24 and T24R cells. These results demonstrate that treating human bladder cancer cells with PT may result in cell cycle arrest that is caused by the down-regulation of cyclins and pRb.

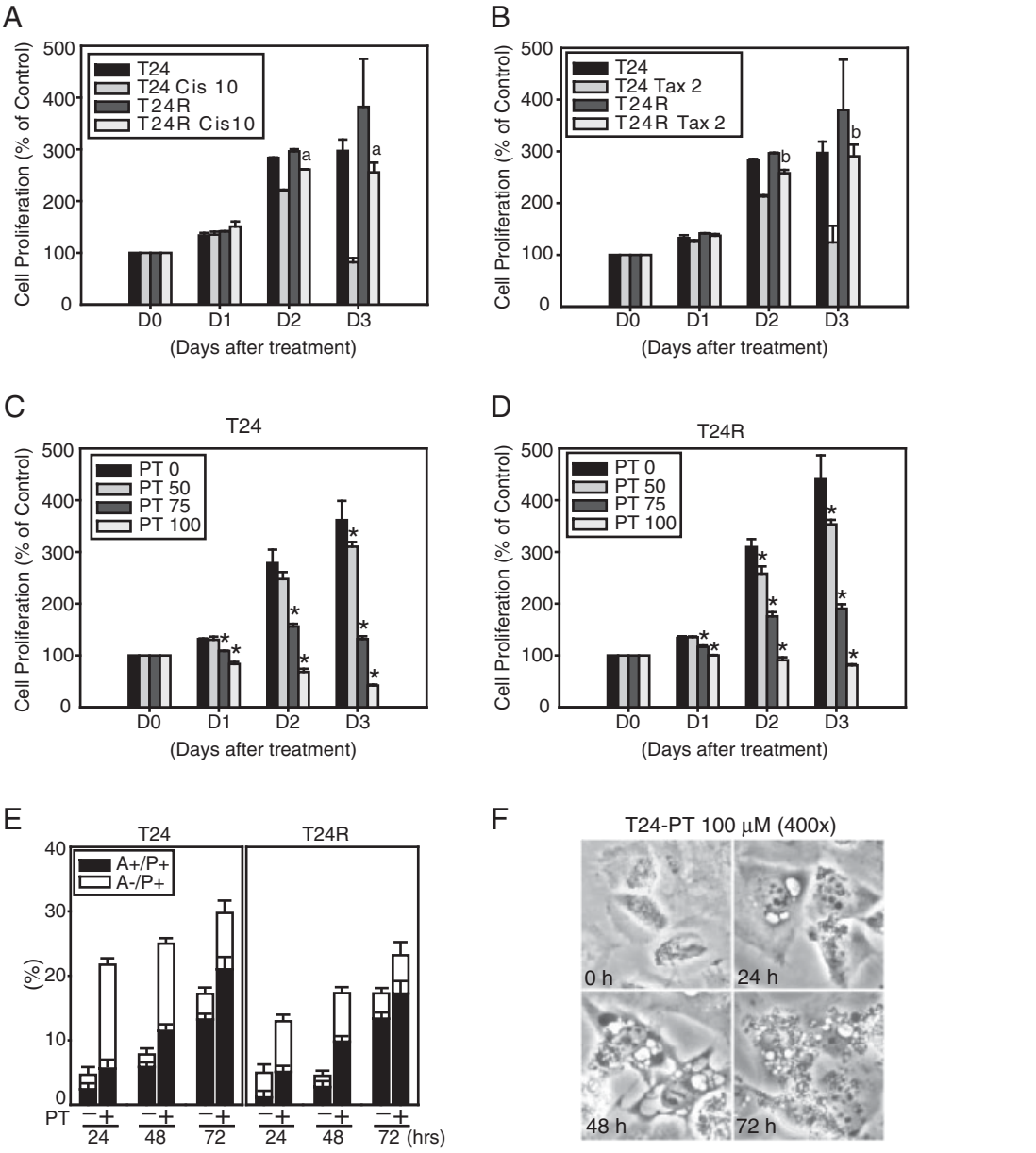

Figure 1. PT inhibits cell proliferation and induces cell death in sensitive and chemoresistant T24 human bladder cancer cells. Cell proliferation rates are compared in sensitive T24 cells and chemoresistant T24 cells (T24R) treated with (A) Cis (10 μM) or (B) paclitaxol (Tax, 2 nM) for 1–3 days. D0: The baseline at which cells were plated and grown for 24 h without treatment. D1, D2, D3: Days after drug treatment for 1, 2 and 3 days. (A) $p<0.05$, T24R Cis 10 *versus* T24 Cis 10. (B) $p<0.05$, T24R Tax 2 *versus* T24 Tax 2. Data represent mean ± SEM of three independent experiments. A570 values of T24 controls are D0: 0.143 ± 0.006, D1: 0.184 ± 0.006, D2: 0.398 ± 0.002, D3: 0.405 ± 0.039. A570 values of T24R controls are D0: 0.143 ± 0.006, D1: 0.198 ± 0.006, D2: 0.410 ± 0.011, D3: 0.532 ± 0.120. PT effectively inhibits cell proliferation in both (C) T24 and (D) T24R cells in a concentration- and time-dependent manner. $^*p<0.05$ compared with PT 0 controls. A570 values of T24 controls are D0: 0.143 ± 0.006, D1: 0.183 ± 0.005, D2: 0.391 ± 0.045, D3: 0.502 ± 0.059. A570 values of T24R controls are D0: 0.143 ± 0.006, D1: 0.187 ± 0.003, D2: 0.431 ± 0.031, D3: 0.598 ± 0.065. The results shown are the mean ± SEM of four independent experiments. (E) Quantification of cell death using the Annexin V-FITC and PI double staining assay. The percentage of dead cells is shown in the bar chart (mean ± SEM of three independent experiments). A+/P+: Annexin V and PI positive; A−/P+: Annexin V negative but PI positive. (F) The morphological changes of T24 cells treated with PT 100 μM for 0, 24, 48 and 72 h were recorded under a phase-contrast microscope (400×).

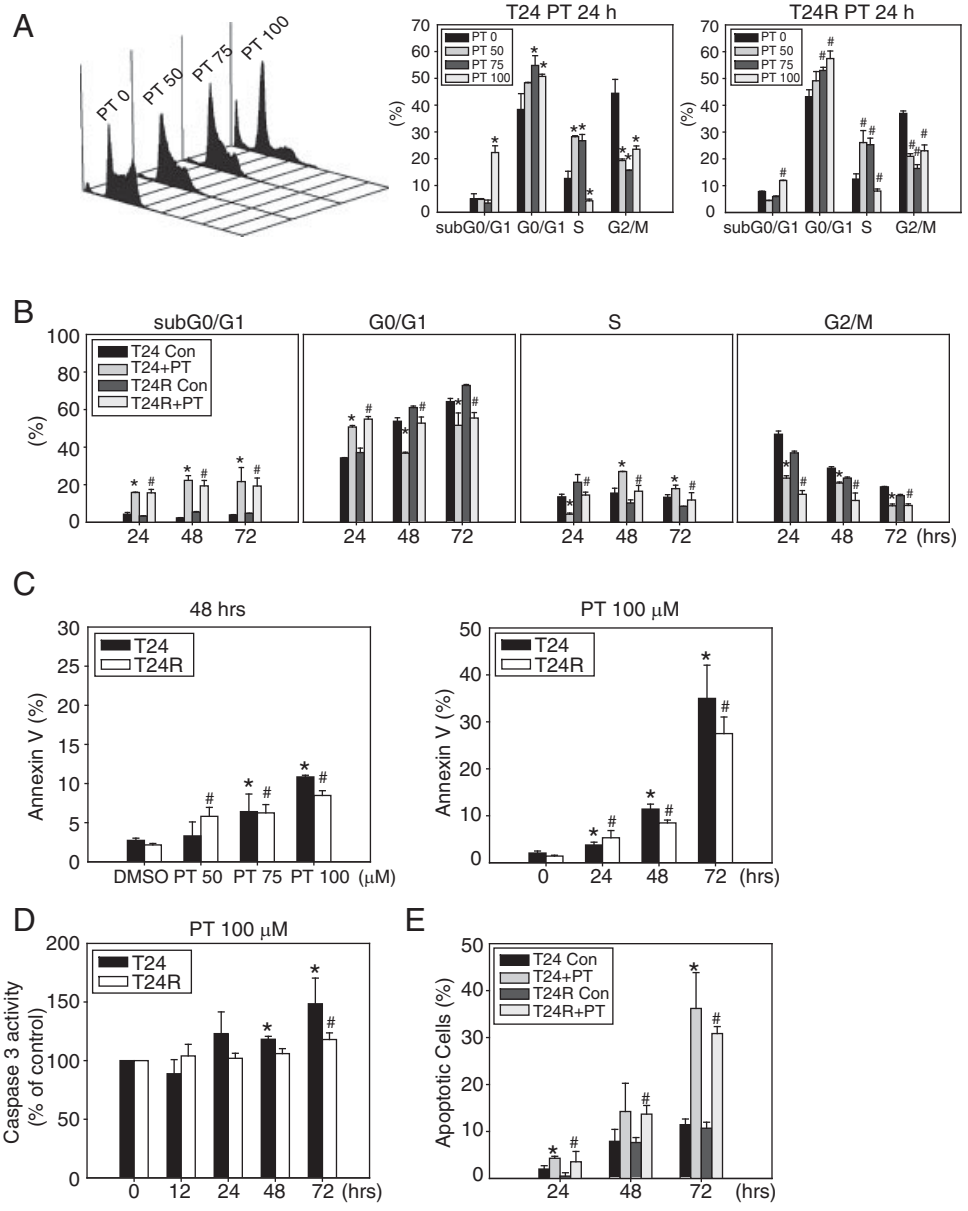

Figure 2. Effects of PT on cell cycle and apoptosis in T24 and T24R bladder cancer cells. Cell cycle analysis was performed by flow cytometry in T24 and T24 R cells treated with PT in a (A) concentration- and (B) time-dependent manner. The data represent the mean ± SEM of three independent experiments; $^{*}p<0.05$ compared with T24 control groups; $^{\#}p<0.05$ compared with T24R control groups. Cells were collected and subjected to the following apoptotic assays: (C) Annexin V staining as a specific apoptosis marker, (D) Caspase-3 activity was detected using a fluorescence spectrophotometer (400 nm excitation and 505 nm emission). The caspase-3 activity values at 0 h are 2170 ± 416.6 and 2400 ± 29.7 for T24 and T24R cells, respectively, (E) the presentative micrographs of DAPI stain are shown in schematic. Bars indicated the percentage of total cells with nuclear condensation and fragmentation, typical characteristics of apoptosis. The data represent the mean ± SEM of three independent experiments; $^{*}p<0.05$ compared with T24 control groups; $^{\#}p<0.05$ compared with T24R control groups.

3.3 PT induces autophagy in bladder cancer cells

Because PT-induced apoptosis was a slow process, and the morphological characteristics changes following treatment (Fig. 1F), we hypothesised that other mechanisms mediate the response to PT. We assessed whether PT induces autophagy in human bladder cancer cells. Autophagic vacuoles containing cellular material or membranous structures were increased in both cell lines treated with PT (100 μM) for 48 h compared with untreated cells, as determined by electron microscopy (Fig. 4A). We used Acridine orange staining to quantify AVOs, including autophagic vacuoles and lysosomes. Cells with AVOs had enhanced red fluorescence that was detected by fluorescence microscopy and flow cytometry (Supporting Information Fig. S2). PT caused AVOs induction in both sensitive and drug-resistant T24 cells in a concentration- (Fig. 4B) and time- (Fig. 4C) dependent manner. Peak AVOs formation occurred at 48 h and decreased at 72 h (Fig. 4C). We next determined the expression of LC3-II by western blotting. The conversion of LC3 from LC3-I (18 kDa cytosolic free form) to LC3-II (16 kDa autophagosomal membrane-bound form) is a key step in the induction of autophagy [26]. A concentration- and time-dependent induction of LC3-II was revealed in both cell lines. As shown in Figs. 4D and E, PT (100 μM) caused a significant increase in LC3-II in both cell lines that is notable in T24 cells from 12 to 48 h.

Bcl-2 and Bcl-xl are anti-apoptotic proteins that also negatively regulate autophagy through interaction with Beclin 1 [27]. PT decreased the protein levels of Bcl-2 and

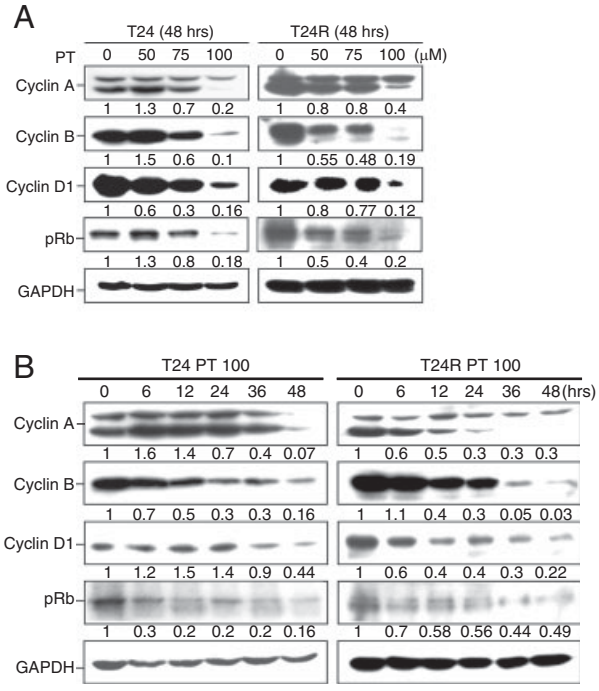

Figure 3. The effects of PT treatment on cell cycle regulatory protein expression in T24 and T24R cells. (A) T24 and T24R cells were treated with various concentrations of PT for 48 h or (B) 100 μM of PT 100 for the indicated times. After treatment, cell lysates were isolated and immunoblotted with anti-Cyclin A, B, and D1, and pRb antibodies. The membrane was probed with anti-GAPDH to confirm equal loading of proteins. Representative data from one of the three independent experiments are shown. The number below each line indicates the relative intensity of protein expression compared with (A) PT 0 control or (B) the PT 100 0 h control (defined as 1).

Bcl-xl in T24 and T24R cells (Figs. 4D and E). PT does not cause significant changes in Bax or Bad expression at 48 h. These findings, combined with the above results, show that autophagy was induced by PT at an earlier stage, and apoptosis occurs at a later stage.

3.4 Autophagy inhibitors increased PT-induced apoptosis in human bladder cancer cells

We used autophagy inhibitors to elucidate the relationship between autophagy and apoptosis induced by PT. The specific autophagy inhibitors were used as follows: (i) 3-MA, a specific class III PI3K inhibitor that prevents early stage autophagy [28] and (ii) BafA1, an inhibitor of vacuolar H^+-ATPase that prevents late stage autophagy by inhibiting fusion of autophagosomes and lysosomes [29]. Cells were pretreated with 3-MA or BafA1 for 1 h before PT treatment. The results showed that AVOs were significantly reduced in the presence of 3-MA or BafA1. Identical data were obtained by inhibiting autophagy with shRNA against *BECN1* because Beclin 1 protein is essential for autophagosome production (Fig. 5B). Western blot analysis demonstrated that transfection with *BECN1* shRNA reduced beclin1 expression by approximately 50%. LC3-II production was reduced in cells pretreated with 3-MA and *BECN1* shRNA, indicating inhibition of the autophagic response, whereas cells pretreated with BafA1 showed accumulation of LC3-II (Fig. 5A). Figure 5C shows increased apoptosis in cells that were pretreated with 3-MA (35%), BafA1 (25%) or *BECN1* shRNA (30%) when compared with control PT-treated groups (18%).

The Z-VAD-FMK pan-caspase inhibitor was used as an apoptosis suppressor to determine whether PT-induced apoptosis killed the cells. Pretreatment with Z-VAD-FMK (20 μM) reduced the percentage cells positive for Annexin V after PT treatment for 72 h (Fig. 5D). Furthermore, cell viability was restored in both cells (Fig. 5E). In contrast, treatment with 3-MA or BafA1 alone reduced the cell viability in both cell types, indicating that theses inhibitors are slightly toxic to cells. The combination of autophagy inhibitors and PT had a synergistic effect on cell death (Fig. 5E). The results indicated that autophagy alone is not sufficient to induce cell death, and PT-induced cell death occurs primarily through apoptosis.

3.5 PT induces autophagy through inhibition of the AKT/mTOR/p70S6K pathway and activation of the MEK/ERK1/2 pathway in T24 cells

The AKT/mTOR/p70S6K pathway is the main pathway that negatively regulates autophagy [30]. mTOR activates the down stream p70S6 Ser/Thr kinase that phosphorylates ribosomal protein S6. Thus, mTOR activity can be monitored by the phosphorylation of p70S6K [31]. The ERK1/2 pathway has been reported to positively regulate autophagy in cancer cells [12]. Therefore, we examined the activation of the AKT/mTOR/p70S6K and ERK1/2 pathways by western blotting. T24 cells treated with PT (75 μM) showed decreased AKT and p70S6K phosphorylation and activation of ERK1/2 for up to 72 h (Fig. 6A). These results indicated that PT inhibits the AKT/mTOR/p70S6K pathway and activates the ERK1/2 pathway and suggests that these changes mediate PT-induced autophagy (Fig. 6A).

We further utilised a PI3K/AKT inhibitor (LY294002) to investigate the role of AKT in down-regulation of autophagy. T24 cells pretreated with LY294002 (10 μM) had increased AVOs induction (74%) (Fig. 6B) and LC3-II expression (Fig. 6B) compared with PT treatment alone (40%). These results indicate that PT-induced autophagy is mediated by inhibition of AKT/mTOR/p70S6K. The MEK1/2 inhibitor (U0126) was used to further confirm the role of the ERK1/2 pathway in PT-induced autophagy. Pretreatment with U0126 (2.5 μM) effectively inhibited induction of AVOs (24%) and production of LC3-II (Fig. 6B) in T24 cells compared with PT alone (45%).

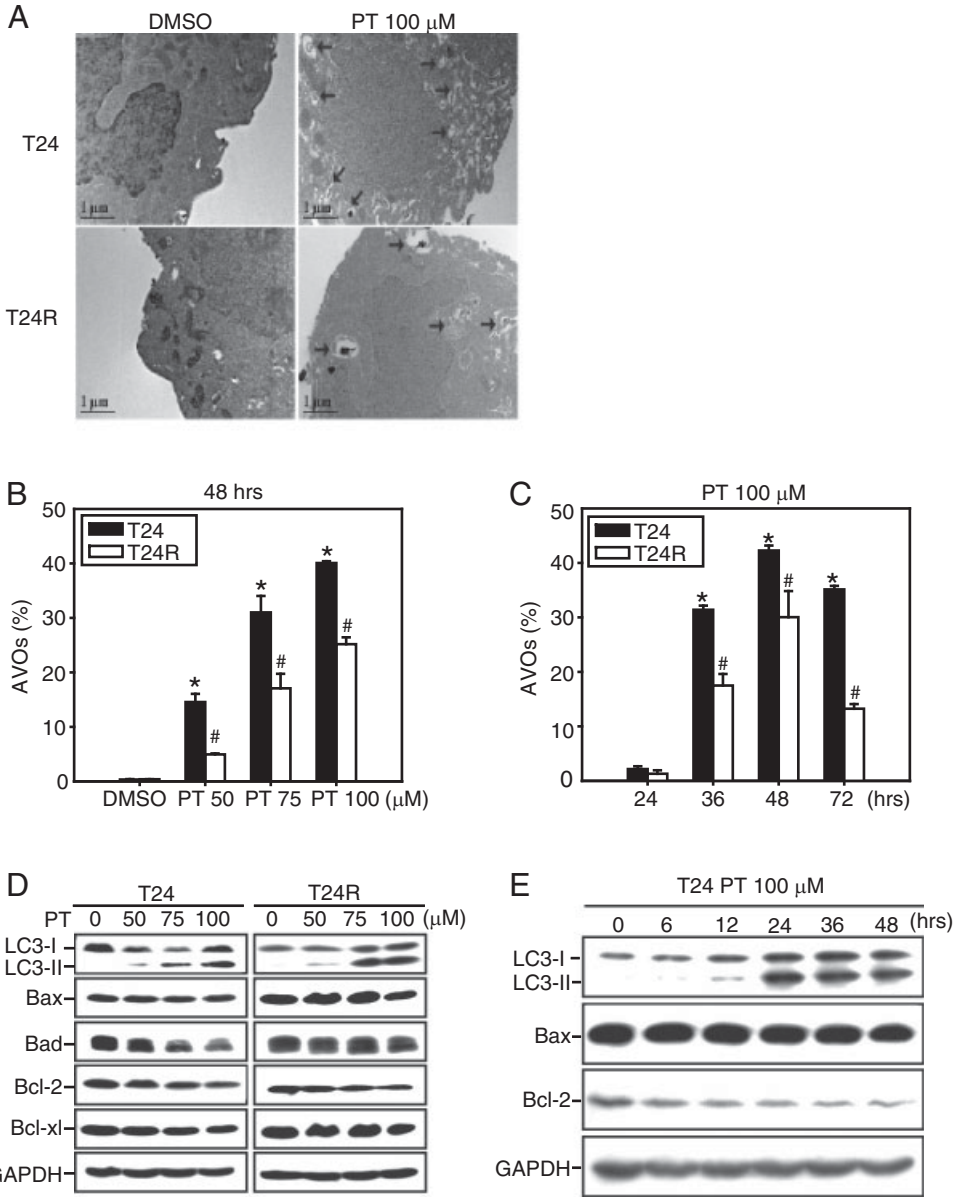

Figure 4. Concentration- and time-dependent autophagic effects of PT in T24 cells. (A) Electron microscope micrographs of T24 cells treated with DMSO or PT for 48 h. The arrows point to autophagic vacuoles and autolysosomes. Bars: 1 μm. T24 and T24R cells were treated with PT in a (B) concentration- and (C) time-dependent manner and stained with acridine orange. The induction of AVOs was detected by flow cytometry. The data represent the mean ± SEM of three independent experiments; $^{*}p < 0.05$ compared with T24 control groups; $^{\sharp}p < 0.05$ compared with T24R control groups. An evident (D) concentration- and (E) time-dependent increase in total LC3 expression and conversion from LC3-I (free form) to LC3-II (membrane-bound form) were revealed in T24 cells and T24R cells. Cell lysates were immunoblotted with specific antibodies to detect Bax and Bad apoptosis regulatory proteins. Bcl-2 and Bcl-xl (negative regulators of autophagy) were also detected by western blotting. The membrane was probed with anti-GAPDH to confirm equal loading of proteins.

We further examined the role of ERK1/2 in PT-induced autophagy by simultaneously transfecting T24 and T24R cells with *ERK1* and *ERK2* shRNA. The ERK1/2 protein expression was reduced to 30% in sh*ERK* groups (Fig. 6C). Transfecting with *ERK1/2* or control shRNA alone increased AVOs compared with control in the absence of PT in both cells (Figs. 6C and D). We suggested that transfection process or PT treatments are variables that affect the AVOs induction. Silencing of *ERK1/2* significantly reduced PT-induced AVOs in T24 (Fig. 6C) and T24R cells (Fig. 6D) and instead increased apoptosis in both cell lines (Figs. 6E and F) when compared with PT alone. Our results confirmed that PT-induced autophagy primarily occurs through inhibition of AKT/mTOR/p70S6K and activation of ERK1/2. We further demonstrated that apoptosis, as detected by DAPI, was increased in T24 cells when autophagy was inhibited by 3-MA, BafA1, *BECN1* shRNA or *ERK1/2* shRNA transfection (Supporting Information Fig. S1B).

4 Discussion

According to the previous studies, the mechanisms by which PT exerts its antitumour effects may include the following: (i) PT is a chemopreventive agent that inhibits herbicide-induced oxidative damage, the expression of COX-2-mediated carcinogenesis [5], iNOS expression and azoxymethane-induced ACF (aberrant crypt foci) preneoplastic lesions in rats [32]; (ii) PT inhibits AGS gastric cancer cell growth by arresting cells in the G0/G1 phase by

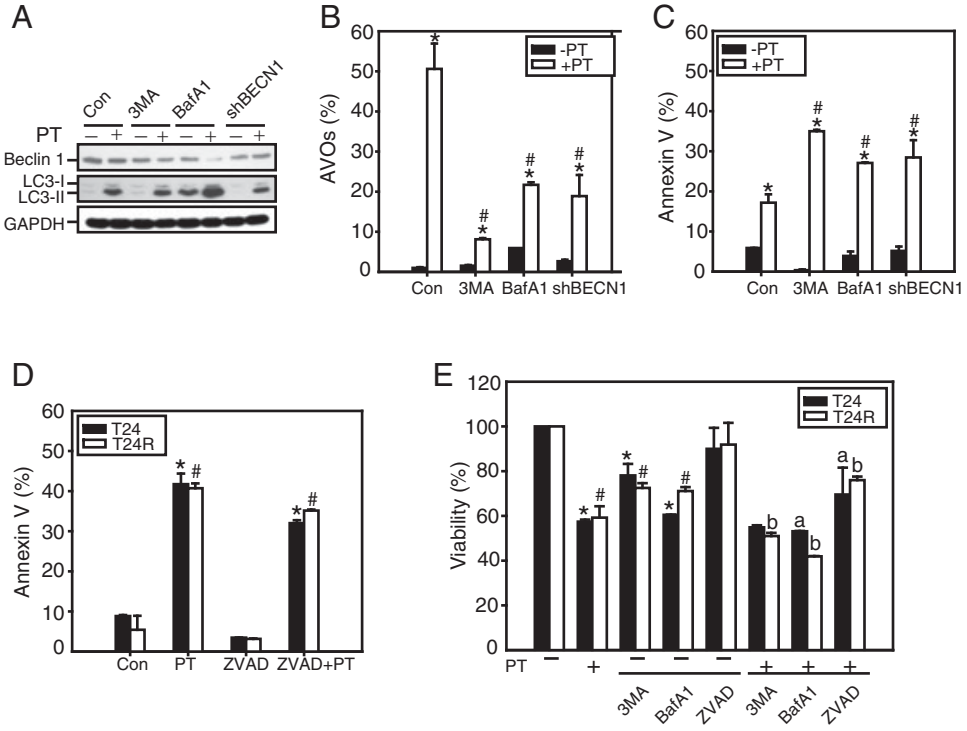

Figure 5. Autophagy inhibition enhanced PT-induced apoptosis in T24 cells. (A) Effects of autophagy inhibitors 3-MA, BafA1 and *BECN1* shRNA on protein expression. Cells were pretreated with 3-MA 5 mM, BafA1 2.5 nM for 1 h, or transfected with *BECN1* shRNA (10 μg) followed by treated with PT 100 μM for 48 h. The protein expression of Beclin 1 and the production of LC3-II were detected by western blotting. (B) The inhibition of AVOs. (C) Induction of Annexin V was determined by flow cytometry. The data represent the mean ± SEM of three independent experiments; $^{*}p<0.05$ compared with each group in the absence of PT; $^{\#}p<0.05$ compared with Con PT-treated groups. (D) Effects of the pan-caspase inhibitor Z-VAD-FMK (20 μM) on PT-induced apoptosis were estimated by Annexin V staining in both cells at 72 h. (E) Effects of 3-MA, BafA1 and Z-VAD-FMK on PT-induced cell death were detected by the MTT assay following a 72 h treatment with PT. mean ± SEM, $n=3$, $^{*}p<0.05$ compared with T24 cells in the absence of PT, $^{\#}p<0.05$ compared with T24R cells in the absence of PT, a: $p<0.05$ compared with T24 cells treated with PT, b: $p<0.05$ compared with T24R cells treated with PT.

up-regulating of p53, p21, p27 and p16, and by down-regulating pRb [33]; (iii) PT induces apoptosis in sensitive and chemoresistant lymphoma cell lines through the caspase-independent pathway [9] and (iv) PT inhibits B16 melanoma growth and metastatic activity. This effect may be regulated by NO accumulation, which inhibit the expression of intracellular adhesion molecules and induces cytotoxicity by increasing Bax expression and decreasing Bcl-2 expression [7]. Pan *et al.* also suggested that PT protects against TPA-mediated metastasis *via* down-regulation of EGF, PKC, PI3K, MAPK and NF-κB pathways and suppression of MMP9 expression [34]. We found that PT-treated cells exhibited antiproliferative effects that were characterised by cell cycle arrest, autophagy and apoptosis. PT inhibited AKT/mTOR/p70S6K and activated ERK1/2 signalling during the process of autophagy.

Our results (Fig. 1E) also indicate that PT induces necrosis followed by autophagy and apoptosis. Previous studies indicate that necrosis and apoptosis are often initiated in response to the same types of insults but by different doses or intensities. Moreover, the features of necrosis and apoptosis may coexist in the same cell [35]. We suggested that T24 and T24R cells suffered from a sudden stress induced by PT may not adapt to the changes thus undergoing necrosis at earlier time point then autophagy and apoptosis occurred. Previous study indicated that necrosis, autophagy and apoptosis may coexist, and the contribution of the three processes can dictate the fate of tumour growth or regression [13]. Thus, although PT results in less autophagy or apoptosis in T24R cells, we suggest that PT is still an effective anti-cancer agent because it limits cancer cell growth through combined anti-cancer effects of necrosis, cell cycle arrest and apoptosis.

PT is commonly found in certain berries and grapes [36]. The levels of PT depend on the types of berries. Some varieties of blueberries contain as much as 15 μg of PT *per* 100 g of blueberries [37]. The doses of PT required to inhibit cancer cell growth may depend on the cell type. For example, PT has an IC_{50} of 4.09 ± 3.05 μg/mL in Hep-G2 cells, an IC_{50} of 10.4 ± 3.8 μg/mL in MDA-MB231 cells, an IC_{50} of 11.6 ± 0.8 μg/mL in HCT-116 cells and an IC_{50} of 108 ± 6 μg/mL in A-357 cells [8]. However, the micro molar concentration of PT is not easily achievable merely by food intake. To enhance PT bioavailability, researches should

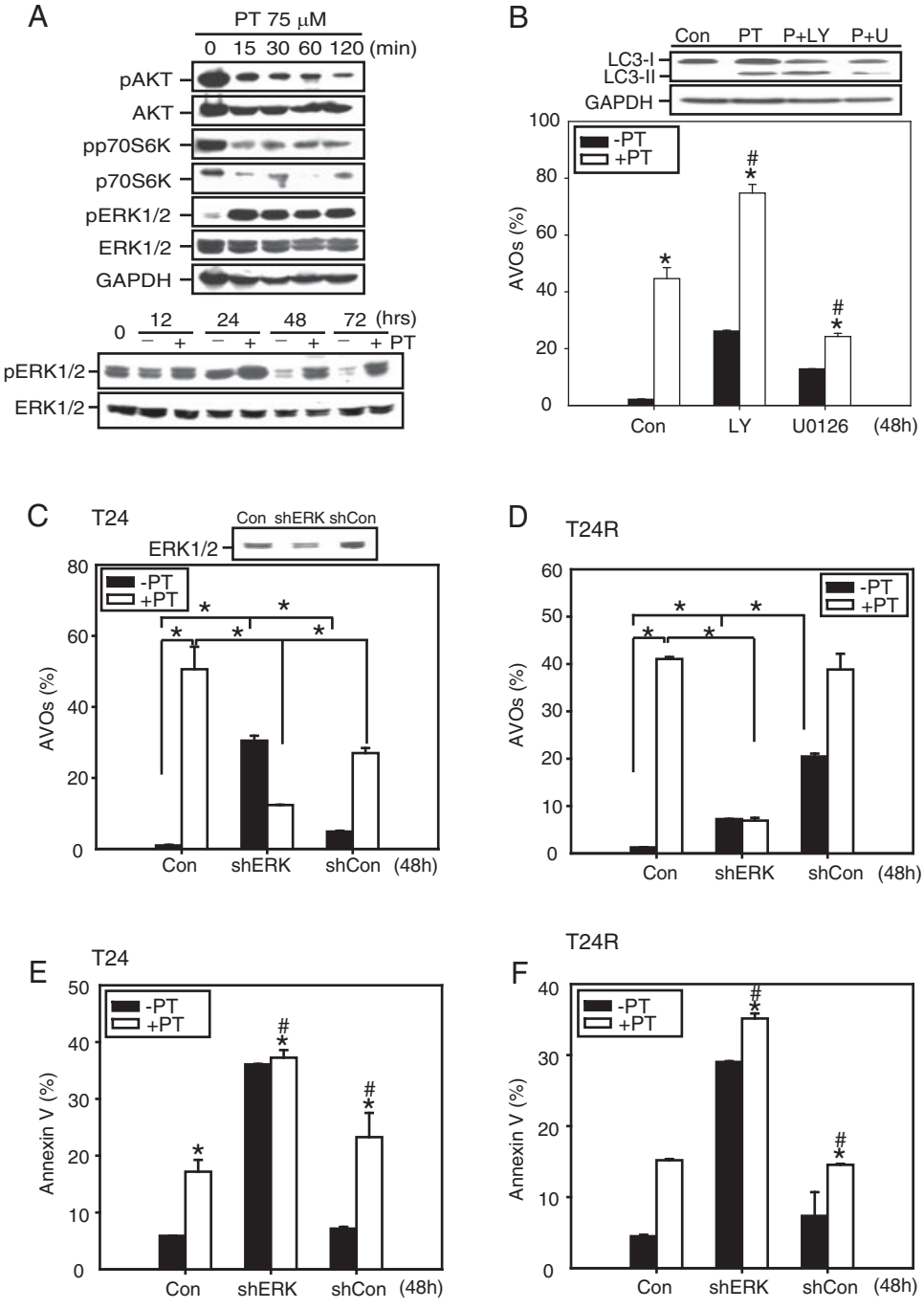

Figure 6. PT-induced autophagy is mediated by inhibition of the AKT/mTOR/p70S6K pathway and activation of the ERK1/2 pathway in T24 cells. (A) The protein levels of pAKT, AKT, pp70S6K, p70S6K, pERK1/2 and ERK1/2 were analysed by western blotting using specific antibodies after treatment with 75 μM PT for the indicated times. (A) PT (100 μM) induced pERK1/2 activation at 12, 24, 48 and 72 h compared with control. (B) Cells were pretreated with LY294002 10 μM or U0126 2.5 μM for 1 h followed by treatment with PT for 48 h. Western blot analysis of LC3-I and LC3-II production used the LC3 antibody. Measurement of AVOs was detected by flow cytometry. T24 cells were transfected with *ERK1* and *ERK2* shRNA (sh*ERK*, 10 μg each) simultaneously or control shRNA (shCon, 10 μg) for 24 h then treated with PT 100 μM for 48 h. The data represent the mean ± SEM of three independent experiments; $^{*}p<0.05$ compared with each group in the absence of PT; $^{\#}p<0.05$ compared with Con PT-treated groups. (C) The reduced autophagy measured by the percentage of AVOs in T24 and (D) T24R cells. Mean ± SEM; $n=3$, $^{*}p<0.05$ analysed by ANOVA. Increased apoptosis determined by Annexin V (E: T24 cells, F: T24R cells) were analyzed by flow cytometry, $^{*}p<0.05$ compared with each group in the absence of PT; $^{\#}p<0.05$ compared with Con PT-treated groups (mean ± SEM; $n=3$).

examine the delivery routes or formulations and modulations of PT metabolism. It will also be important to examine potential interactions of PT with other food components, biotherapy, cytotoxic agents, and/or ionizing radiation used to treat malignant tumours.

We found that PT inhibits the proliferation and survival of sensitive and drug-resistant bladder cancer cell lines. Cell cycle analysis demonstrated that PT induces a G0/G1 phase arrest and decreases the percentage of cells in G2/M phases after a 24 h exposure. These results are consistent with other reports showing that PT induces a G0/G1 arrest in CEM-C7H2 leukaemia cells [9]. Pan *et al.* showed that PT exerts growth inhibition by inducing apoptosis and arresting gastric cancer cells in the G0/G1 phase [33]. The relationship between autophagy and cell cycle progression is not yet clear. A variety of agents have been reported to induce autophagy in association with G2/M cell cycle arrest [20]. Autophagy may be relevant for recycling the proteins

necessary for negative cell cycle regulation. Thus, such proteins would not be available when autophagy decreases, and progression through the cell cycle would increase [38]. These studies suggest that the role of autophagy may be connected with cell cycle regulation. We found that the antiproliferative effects of PT correlated with a G1 arrest in a dose-dependent manner, and the percentage of cells in G2/M and S-phase was decreased. The G1 arrest may be associated with the time-dependent decrease in the Cyclin D1, Cyclin A and Cyclin B cell cycle regulatory proteins. Phosphorylation of Rb was significantly reduced at 6 h, which was earlier than other proteins (Fig. 3B). This suggested that other factors upstream of Rb could be affected by PT at an earlier time point. White suggested that rapamycin, an autophagy inducer that inhibits mTOR, reduces Rb phosphorylation by modulating the stability and expression of Cyclin D1 and p27 [39]. Moreover, rapamycin inhibits rRNA synthesis that involves the Rb protein [40]. These studies indicate that phosphorylation of Rb could be reduced by inactivation of mTOR. Our results showed that the AKT/mTOR pathway was inactivated within 15 min following PT treatment (Fig. 6A). We postulate that the PT-induced reduction in pRb may contribute to inhibition of mTOR.

Autophagy has attracted the interest of scientists in the cancer therapy field because drug-resistant cancer cells with antiapoptotic properties may be vulnerable to death by autophagy. The results obtained in this study indicate that PT is active as an autophagy-inducing agent in sensitive and Cis/Tax-resistant bladder cancer cells. Similar to PT, resveratrol, an analogue of PT, induces autophagy in ovarian and drug-resistant breast cancer cells [41, 42]. In our study, pterostilben-induced autophagy is not sufficient by it self to induce cell death. After a latency period, PT induces cell death *via* apoptosis. In addition, inhibition of autophagy by 3-MA or BafA1 may increase the sensitivity of cells to death signals. Consistent with our results, Abedin *et al.* found that inhibition of autophagy increases mitochondria depolarisation and apoptosis in camptothecin-treated MCF-7 cells [43]. Similarly, other reports show that cell death is enhanced by autophagy inhibitors that increase the sensitivity of cells to apoptosis [44, 45]. Our results suggest that autophagy is a dominant mechanism in T24 cells treated with PT, but additional cell death may occur when autophagic cells have apoptotic features. This suggests an overlap or interdependence between these cell death programs. BafA1 inhibits the formation of autophagolysosomes through the fusion of autophagosomes and lysosomes. This reduces autophagosomes turnover and lead to abnormal AVO's accumulation and insufficient clearance of LC3-II proteins [29]. Abnormal autophagosomes accumulation can enhance cell death by BafA1 treatment alone and in combination of PT (Fig. 5E). Similarly, blocking the class III PI3K by 3-MA inhibits the formation of autophagosomes and sensitises cells to PT-induced apoptosis and cell death (Fig. 5E). 3-MA may affect other targets, including class I PI3K, p38, JNK or the mitochondria permeability transition to enhance cytotoxicity [46]. Such autophagy inhibitors that modulate cell death may be not properly used to prove whether autophagy is involved in lethal processes.

This study clearly demonstrated that PT inhibits the AKT/mTOR/p70S6K and activates the ERK1/2 pathway to promote autophagy. Blocking PI3K/AKT signalling with LY294002 enhances the AVO induction and LC3-II production induced by PT. Ellington *et al.* showed that the natural product triterpenoid B-group soy saponins induced autophagy by inhibiting AKT and activating ERK activity [47]. Our recent report showed that a combination of arsenic trioxide and irradiation enhances autophagic effects in glioma cells through the inhibition of AKT and activation of ERK1/2 signalling [12]. These findings may highlight the common mechanisms, such as AKT inhibition and ERK1/2 activation that regulate autophagy in cancer cells treated with anticancer agents. Interestingly, T24 cells treated with the highly selective MEK1/2 inhibitor U0126 led to a slight induction of autophagy (10%) (Fig. 6B). Fukazawa *et al.* found that U0126 reduced activation of ERK and p70S6K (downstream of mTOR) in MDA-MB231 and HBC4 cells [48]. We suggest that U0126 alone could induce autophagy in T24 cells by influencing mTOR signalling. We further confirmed the role of ERK1/2 in autophagy by simultaneously transfecting with *ERK1* and *ERK2* shRNA. However, sh*ERK1/2* alone induced 30% of AVOs in T24 cells. Transfection with a high dose of *ERK1* and *ERK2* shRNA (10 μg each) may increase cellular stress that leads to autophagy without PT treatment. Similar effects were observed in cells transfected with control shRNA (shCon) (Figs. 6C and D). Previous studies suggest that some transfection techniques cause a cellular stress response [49, 50]. Cells undergoing a stress response may induce cell damage and cause cell death through apoptosis, necrosis or autophagy [50, 51]. According to the MicroPorator protocol, cells have to grow in serum-free conditions after transfection, and that is a well-known inducer of autophagy [51]. Thus, we suggest that electroporation may also induce cellular stress that cause autophagy under specific growth conditions. However, the mechanisms regulating autophagy induced by transfection remain further studied. In addition, both U0126 and sh*ERK1/2* partially inhibited autophagy (Figs. 6B and C), indicating that MEK/ERK1/2 is not the only pathway that induces autophagy in T24 cells. Other mechanisms, such as the AMPK, the physical cellular energy sensor [52], may regulate autophagy in T24 cells. Nevertheless, apoptosis was increased in *ERK1/2* shRNA groups, and this is further confirmation that inhibition of autophagy sensitises the cells to apoptosis.

Several signals that are triggered by cellular stresses can elicit both autophagy and apoptosis. For example, Bcl-2 family proteins are important regulators of apoptosis, and there is increasing evidence that Bcl-2 family proteins can also regulate autophagy. Distinct regions of Beclin 1 are involved in binding to Vsp34 and to Bcl-2/Bcl-xl in human

cancer cells [53]. Bcl-2 or Bcl-xl binds to Beclin 1 and disrupts its interaction with Vsp34. This results in decreased Vsp34/PI3K activity and inhibition of autophagy in certain conditions [54]. Down-regulation of Bcl-2 increases autophagy in leukaemia cells [55]. The relationship between Bcl-2 and autophagy is not fully understood, but it is likely that the interaction between Bcl-2 and Beclin 1 may be a turning point between cell survival and death [27, 56].

Cancer cells are initially sensitive to apoptotic induction, but become resistant through deregulation of apoptosis. Agents that kill cancer cells through nonapoptotic pathways may circumvent this drug resistance [15]. Thus, there is growing interest in the anticancer therapy field to search for novel compounds that induce autophagy. We determined the optimal antiproliferative effects of PT in sensitive and nicotine-induced chemoresistant human bladder cancer cells. We demonstrated that anti-cancer effects of PT are regulated by autophagy, apoptosis and cell cycle arrest, and the signalling pathways mediating PT-induced autophagy were identified. To the best of our knowledge, the study is the first to demonstrate that PT can promote autophagy in both chemosensitive and chemoresistant bladder cancer cells. In conclusion, PT possesses an interesting autophagy-inducing property, and autophagy inhibitors may enhance cytotoxicity in both chemosensitive and chemoresistant bladder cancer cells.

This work was supported by National Science Council (NSC 98-2314-B-006-034-MY2).

The authors have declared no conflict of interest.

5 References

[1] Sengupta, N., Siddiqui, E., Mumtaz, F. H., Cancers of the bladder. *J. R. Soc. Promot. Health* 2004, *124*, 228–229.

[2] Dreicer, R., Locally advanced and metastatic bladder cancer. *Curr. Treat. Opt. Oncol.* 2001, *2*, 431–436.

[3] Fleshner, N., Garland, J., Moadel, A., Herr, H. *et al.*, Influence of smoking status on the disease-related outcomes of patients with tobacco-associated superficial transitional cell carcinoma of the bladder. *Cancer* 1999, *86*, 2337–2345.

[4] Chen, R. J., Ho, Y. S., Guo, H. R., Wang, Y. J., Long-term nicotine exposure-induced chemoresistance is mediated by activation of stat3 and downregulation of ERK1/2 *via* nAChR and beta-AR in human bladder cancer cells. *Toxicol. Sci.* 2010, *115*, 118–130.

[5] Rimando, A. M., Cuendet, M., Desmarchelier, C., Mehta, R. G. *et al.*, Cancer chemopreventive and antioxidant activities of pterostilbene, a naturally occurring analogue of resveratrol. *J. Agric. Food Chem.* 2002, *50*, 3453–3457.

[6] Stivala, L. A., Savio, M., Carafoli, F., Perucca, P. *et al.*, Specific structural determinants are responsible for the antioxidant activity and the cell cycle effects of resveratrol. *J. Biol. Chem.* 2001, *276*, 22586–22594.

[7] Ferrer, P., Asensi, M., Segarra, R., Ortega, A. *et al.*, Association between pterostilbene and quercetin inhibits metastatic activity of B16 melanoma. *Neoplasia* 2005, *7*, 37–47.

[8] Remsberg, C. M., Yanez, J. A., Ohgami, Y., Vega-Villa, K. R. *et al.*, Pharmacometrics of pterostilbene: preclinical pharmacokinetics and metabolism, anticancer, anti-inflammatory, antioxidant and analgesic activity. *Phytother. Res.* 2008, *22*, 169–179.

[9] Tolomeo, M., Grimaudo, S., Di Cristina, A., Roberti, M. *et al.*, Pterostilbene and 3′-hydroxypterostilbene are effective apoptosis-inducing agents in MDR and BCR-ABL-expressing leukemia cells. *Int. J. Biochem. Cell Biol.* 2005, *37*, 1709–1726.

[10] Kroemer, G., Jaattela, M., Lysosomes and autophagy in cell death control. *Nat. Rev. Cancer* 2005, *5*, 886–897.

[11] Yorimitsu, T., Klionsky, D. J., Autophagy: molecular machinery for self-eating. *Cell Death Diff.* 2005, *12*, 1542–1552.

[12] Chiu, H. W., Ho, S. Y., Guo, H. R., Wang, Y. J., Combination treatment with arsenic trioxide and irradiation enhances autophagic effects in U118-MG cells through increased mitotic arrest and regulation of PI3K/Akt and ERK1/2 signaling pathways. *Autophagy* 2009, *5*, 472–483.

[13] Amaravadi, R. K., Thompson, C. B., The roles of therapy-induced autophagy and necrosis in cancer treatment. *Clin. Cancer Res.* 2007, *13*, 7271–7279.

[14] Mathew, R., Karantza-Wadsworth, V., White, E., Role of autophagy in cancer. *Nat. Rev. Cancer* 2007, *7*, 961–967.

[15] Ruefli, A. A., Smyth, M. J., Johnstone, R. W., HMBA induces activation of a caspase-independent cell death pathway to overcome P-glycoprotein-mediated multidrug resistance. *Blood* 2000, *95*, 2378–2385.

[16] Degenhardt, K., Mathew, R., Beaudoin, B., Bray, K. *et al.*, Autophagy promotes tumor cell survival and restricts necrosis, inflammation, and tumorigenesis. *Cancer Cell* 2006, *10*, 51–64.

[17] Thorburn, A., Apoptosis and autophagy: regulatory connections between two supposedly different processes. *Apoptosis* 2008, *13*, 1–9.

[18] Levine, B., Deretic, V., Unveiling the roles of autophagy in innate and adaptive immunity. *Nat. Rev. Immunol.* 2007, *7*, 767–777.

[19] Klionsky, D. J., Emr, S. D., Autophagy as a regulated pathway of cellular degradation. *Science* 2000, *290*, 1717–1721.

[20] Aoki, H., Takada, Y., Kondo, S., Sawaya, R. *et al.*, Evidence that curcumin suppresses the growth of malignant gliomas *in vitro* and *in vivo* through induction of autophagy: role of Akt and extracellular signal-regulated kinase signaling pathways. *Mol. Pharmacol.* 2007, *72*, 29–39.

[21] Corcelle, E., Nebout, M., Bekri, S., Gauthier, N. *et al.*, Disruption of autophagy at the maturation step by the carcinogen lindane is associated with the sustained mitogen-activated protein kinase/extracellular signal-regulated kinase activity. *Cancer Res.* 2006, *66*, 6861–6870.

[22] Galluzzi, L., Aaronson, S. A., Abrams, J., Alnemri, E. S. *et al.*, Guidelines for the use and interpretation of assays for

monitoring cell death in higher eukaryotes. *Cell Death Diff.* 2009, *16*, 1093–1107.

[23] Paglin, S., Hollister, T., Delohery, T., Hackett, N. *et al.*, A novel response of cancer cells to radiation involves autophagy and formation of acidic vesicles. *Cancer Res.* 2001, *61*, 439–444.

[24] Kanzawa, T., Kondo, Y., Ito, H., Kondo, S. *et al.*, Induction of autophagic cell death in malignant glioma cells by arsenic trioxide. *Cancer Res.* 2003, *63*, 2103–2108.

[25] Lee, W. S., Chen, R. J., Wang, Y. J., Tseng, H. *et al.*, *In vitro* and *in vivo* studies of the anticancer action of terbinafine in human cancer cell lines: G0/G1 p53-associated cell cycle arrest. *Int. J. Cancer* 2003, *106*, 125–137.

[26] Kabeya, Y., Mizushima, N., Ueno, T., Yamamoto, A. *et al.*, LC3, a mammalian homologue of yeast Apg8p, is localized in autophagosome membranes after processing. *EMBO J.* 2000, *19*, 5720–5728.

[27] Pattingre, S., Tassa, A., Qu, X., Garuti, X. R. *et al.*, Bcl-2 antiapoptotic proteins inhibit Beclin 1-dependent autophagy. *Cell* 2005, *122*, 927–939.

[28] Zhang, X. D., Wang, Y., Zhang, X., Han, R. *et al.*, p53 mediates mitochondria dysfunction-triggered autophagy activation and cell death in rat striatum. *Autophagy* 2009, *5*, 339–350.

[29] Shacka, J. J., Klocke, B. J., Shibata, M., Uchiyama, Y. *et al.*, Bafilomycin A1 inhibits chloroquine-induced death of cerebellar granule neurons. *Mol. Pharmacol.* 2006, *69*, 1125–1136.

[30] Roca, H., Varsos, Z., Pienta, K. J., CCL2 protects prostate cancer PC3 cells from autophagic death *via* phosphatidylinositol 3-kinase/AKT-dependent survivin up-regulation. *J. Biol. Chem.* 2008, *283*, 25057–25073.

[31] Levine, B., Kroemer, G., Autophagy in aging, disease and death: the true identity of a cell death impostor. *Cell Death Diff.* 2009, *16*, 1–2.

[32] Suh, N., Paul, S., Hao, X., Simi, B. *et al.*, Pterostilbene, an active constituent of blueberries, suppresses aberrant crypt foci formation in the azoxymethane-induced colon carcinogenesis model in rats. *Clin. Cancer Res.* 2007, *13*, 350–355.

[33] Pan, M. H., Chang, Y. H., Badmaev, V., Nagabhushanam, K. *et al.*, Pterostilbene induces apoptosis and cell cycle arrest in human gastric carcinoma cells. *J. Agric. Food Chem.* 2007, *55*, 7777–7785.

[34] Pan, M. H., Chiou, Y. S., Chen, W. J., Wang, J. M. *et al.*, Pterostilbene inhibited tumor invasion *via* suppressing multiple signal transduction pathways in human hepatocellular carcinoma cells. *Carcinogenesis* 2009, *30*, 1234–1242.

[35] Zong, W. X., Thompson, C. B., Necrotic death as a cell fate. *Genes Dev.* 2006, *20*, 1–15.

[36] Baur, J. A., Sinclair, D. A., Therapeutic potential of resveratrol: the *in vivo* evidence. *Nat. Rev. Drug Discov.* 2006, *5*, 493–506.

[37] Rimando, A. M., Kalt, W., Magee, J. B., Dewey, J. *et al.*, Resveratrol, pterostilbene, and piceatannol in vaccinium berries. *J. Agric. Food Chem.* 2004, *52*, 4713–4719.

[38] Cecconi, F., Levine, B., The role of autophagy in mammalian development: cell makeover rather than cell death. *Dev. Cell* 2008, *15*, 344–357.

[39] White, R. J., Regulation of RNA polymerases I and III by the retinoblastoma protein: a mechanism for growth control? *Trends Biochem. Sci.* 1997, *22*, 77–80.

[40] Leicht, M., Simm, A., Bertsch, G., Hoppe, J., Okadaic acid induces cellular hypertrophy in AKR-2B fibroblasts: involvement of the p70S6 kinase in the onset of protein and rRNA synthesis. *Cell Growth Differ.* 1996, *7*, 1199–1209.

[41] Opipari, A. W., Jr., Tan, L., Boitano, A. E., Sorenson, D. R. *et al.*, Resveratrol-induced autophagocytosis in ovarian cancer cells. *Cancer Res.* 2004, *64*, 696–703.

[42] Scarlatti, F., Maffei, R., Beau, I., Codogno, P. *et al.*, Role of non-canonical Beclin 1-independent autophagy in cell death induced by resveratrol in human breast cancer cells. *Cell Death Diff.* 2008, *15*, 1318–1329.

[43] Abedin, M. J., Wang, D., McDonnell, M. A., Lehmann, U. *et al.*, Autophagy delays apoptotic death in breast cancer cells following DNA damage. *Cell Death Diff.* 2007, *14*, 500–510.

[44] Amaravadi, R. K., Yu, D., Lum, J. J., Bui, T. *et al.*, Autophagy inhibition enhances therapy-induced apoptosis in a Myc-induced model of lymphoma. *J. Clin. Invest.* 2007, *117*, 326–336.

[45] Longo, L., Platini, F., Scardino, A., Alabiso, O. *et al.*, Autophagy inhibition enhances anthocyanin-induced apoptosis in hepatocellular carcinoma. *Mol. Cancer Ther.* 2008, *7*, 2476–2485.

[46] Kroemer, G., Levine, B., Autophagic cell death: the story of a misnomer. *Nat. Rev. Mol. Cell Biol.* 2008, *9*, 1004–1010.

[47] Ellington, A. A., Berhow, M. A., Singletary, K. W., Inhibition of Akt signaling and enhanced ERK1/2 activity are involved in induction of macroautophagy by triterpenoid B-group soyasaponins in colon cancer cells. *Carcinogenesis* 2006, *27*, 298–306.

[48] Fukazawa, H., Noguchi, K., Murakami, Y., Uehara, Y., Mitogen-activated protein/extracellular signal-regulated kinase kinase (MEK) inhibitors restore anoikis sensitivity in human breast cancer cell lines with a constitutively activated extracellular-regulated kinase (ERK) pathway. *Mol. Cancer Ther.* 2002, *1*, 303–309.

[49] Andrews, J. M., Newbound, G. C., Lairmore, M. D., Transcriptional modulation of viral reporter gene constructs following induction of the cellular stress response. *Nucleic Acids Res.* 1997, *25*, 1082–1084.

[50] Pinero, J., Lopez-Baena, M., Ortiz, T., Cortes, F., Apoptotic and necrotic cell death are both induced by electroporation in HL60 human promyeloid leukaemia cells. *Apoptosis* 1997, *2*, 330–336.

[51] Uchiyama, Y., Shibata, M., Koike, M., Yoshimura, K. *et al.*, Autophagy-physiology and pathophysiology. *Histochem. Cell. Biol.* 2008, *129*, 407–420.

[52] Poels, J., Spasic, M. R., Callaerts, P., Norga, K. K., Expanding roles for AMP-activated protein kinase in neuronal survival and autophagy. *Bioessays* 2009, *31*, 944–952.

[53] Furuya, N., Yu, J., Byfield, M., Pattingre, S. *et al.*, The evolutionarily conserved domain of Beclin 1 is required for Vps34 binding, autophagy and tumor suppressor function. *Autophagy* 2005, *1*, 46–52.

[54] Levine, B., Sinha, S., Kroemer, G., Bcl-2 family members: dual regulators of apoptosis and autophagy. *Autophagy* 2008, *4*, 600–606.

[55] Saeki, K., Yuo, A., Okuma, E., Yazaki, Y. *et al.*, Bcl-2 down-regulation causes autophagy in a caspase-independent manner in human leukemic HL60 cells. *Cell Death Differ.* 2000, *7*, 1263–1269.

[56] Maiuri, M. C., Le Toumelin, G., Criollo, A., Rain, J. C. *et al.*, Functional and physical interaction between Bcl-X(L) and a BH3-like domain in Beclin-1. *EMBO J.* 2007, *26*, 2527–2539.

